

Srijan Datta

Department of Electrical and Computer
Engineering,
Michigan State University,
428 N Shaw Lane,
East Lansing, MI 48824
e-mail: dattasri@egr.msu.edu

Xiaodong Shi

Department of Electrical and Computer
Engineering,
Michigan State University,
428 N Shaw Lane,
East Lansing, MI 48824
e-mail: shixiaod@msu.edu

Saptarshi Mukherjee

Lawrence Livermore National Lab,
Atmospheric, Earth and Energy Division,
7000 East Ave.,
Livermore, CA 94550-9234
e-mail: mukherjee5@llnl.gov

Yiming Deng

Department of Electrical and Computer
Engineering,
Michigan State University,
428 N Shaw Lane,
East Lansing, MI 48824
e-mail: dengyimi@egr.msu.edu

Lalita Udupa

Department of Electrical and Computer
Engineering,
Michigan State University,
428 N Shaw Lane,
East Lansing, MI 48824
e-mail: udpal@egr.msu.edu

Model-Based Study of a Metamaterial Lens for Nondestructive Evaluation of Composites

Composites are being increasingly used in various industries due to their lower cost and superior mechanical properties over traditional materials. They are nevertheless vulnerable to various defects during manufacturing or usage which can cause failure of critical engineering structures. Hence, there is a growing need for nondestructive evaluation (NDE) of composites to detect such defective structures and avoid significant loss and damages. Microwave NDE has several advantages over other existing NDE techniques for detecting defects or faults in non-conducting composites or dielectrics. One of the primary benefits of microwaves is large probe-standoff distances which allow for rapid scan times. However, the resolution of such far-field microwave sensors is diffraction limited. Metamaterial-based lens, also known as "superlens," can achieve resolution beyond the diffraction limits due to its unique electromagnetic (EM) properties. This contribution focuses on the physical design of a metamaterial lens. The theory underlying the design of a metamaterial lens is presented followed by simulation and experimental results. This paper also investigates the feasibility of using the metamaterial lens for improving the resolution of microwave imaging in NDE of composites. [DOI: 10.1115/1.4047027]

Keywords: *metamaterials, electromagnetics, numerical analysis, superlens*

Introduction

Natural fiber-reinforced composites have gained large attraction over the past few years by engineers, academicians, and researchers alike due to their lower cost, preferable mechanical properties, and environmental sustainability over conventional materials such as metals and synthetic fibers. Composites can be tailored to have enhanced characteristics that have facilitated their growing application in industries such as aerospace, automotive, and structural engineering [1–3].

However, composites are susceptible to defects due to manufacturing issues or damages incurred in usage. Two common types of defects in composites are disbonds and delaminations. Disbonds occur when two adhesively joined composites are separated at the bonding joint. Delaminations are caused when two adjacent layers in a laminate are displaced under loading. Hence, there is a need for nondestructive evaluation (NDE) sensors for composites that can reliably detect these flaws that can affect the performance of crucial engineering structures [4,5].

Microwave NDE is the method of using high-frequency electromagnetic (EM) signals to interact with structures and inspect them for vulnerabilities [6]. Microwaves occupy 300 MHz (wavelength of 1 m) to 300 GHz (wavelength of 1 mm) of the EM spectrum.

They have the ability to penetrate deep into low loss dielectrics and hence are suitable for inspection of electrically insulated low loss composites that are replacing metals in many applications [7]. In addition to this, a microwave NDE system offers various advantages over other existing NDE techniques such as non-contact, no requirement for couplants, relatively low cost, and one-sided scanning [8].

Microwaves fundamentally work in two modes, namely near-field (distances typically less than a wavelength from the source) and far-field (distances generally more than two wavelengths) [9]. Far-field microwave sensor systems have advantages of rapid scan time and hence fast detection of large areas of composites. However, the spatial resolution of far-field microwave imaging is limited due to the imposition of the diffraction limits [10]. Near-field microwave sensor systems have a better spatial resolution, but the probe stand-off distance is very small leading to large scanning time, which can be an issue for practical implementations [11]. A metamaterial-based lens, also called a superlens, when used in a microwave NDE setup, combines the advantages of both near-field and far-field modes of operation. The unique EM properties of metamaterial allow the superlens to overcome limits imposed by diffraction [12–14]. This phenomenon can be exploited to build a microwave NDE system that provides rapid scanning at large stand-off distances as well as enhanced spatial resolution. While research on the metamaterial lens has been extensive over the past decade, their implementation for NDE has been relatively less. Although there are works that have used "metamaterials" for NDE [15,16], these systems enhance the image resolution by combining the

Manuscript received October 25, 2019; final manuscript received April 6, 2020; published online May 15, 2020. Assoc. Editor: Shiv Joshi.

proposed metamaterials in the near field region. Hence, the advantages of fast scan time offered by a far-field microwave setup are not utilized in these works. To the authors' best knowledge, the only prior work on the metamaterial lens for NDE has been done by Shreiber et al. [17]. Recent computational modeling involving homogenization of the lens with plasma EM equations has demonstrated the ability to increase the sensitivity for microwave defect imaging in glass fiber-reinforced polymer composites [18]. However, such a homogenized model of the lens does not take into account different EM interactions between the building blocks of an actual metamaterial lens. This paper builds on the work in Ref. [18] by studying the physical model of such a metamaterial lens design. The theory underlying metamaterials is first discussed. Numerical studies to analytically determine the EM properties of the lens are presented subsequently. Further, a lens was fabricated for experimental validation of the numerical studies and initial experimental results for enhancing microwave detection capability are presented.

Metamaterial Lens

Artificially manufactured periodic structures with unusual EM properties that are not readily available in nature are known as metamaterials. The distinctive EM properties used in this work are simultaneous negative permittivity and permeability, which results in a negative refractive index for a given material. Equation (1) gives the relationship between refractive index n , permittivity ϵ , and permeability μ for such metamaterials.

$$n = -\sqrt{\mu \epsilon} \quad (1)$$

The negative refractive index gives rise to unique physical phenomena inside such a material such as reversal of Snell's law, enhancement of evanescent waves, the reversal of Doppler effect, and reversed Cherenkov radiation [19]. The effect of the reversal of Snell's law can be demonstrated in Fig. 1. When a point source is placed in front of a lens of appropriate thickness with refractive index $n = -1$, the waves are refracted in such a way so that the waves focus once inside the lens and then outside the lens. The relationship between the distance of the source from lens d_1 , focusing distance d_2 and thickness of the lens t for the metamaterial lens with refractive index equals to -1 can be expressed as

$$d_1 + d_2 = t \quad (2)$$

Additionally, the amplitude of the evanescent wave that contains the high spatial frequency information amplifies inside the metamaterial lens. While the evanescent waves decay exponentially over the direction of propagation and hence not transmitted in a

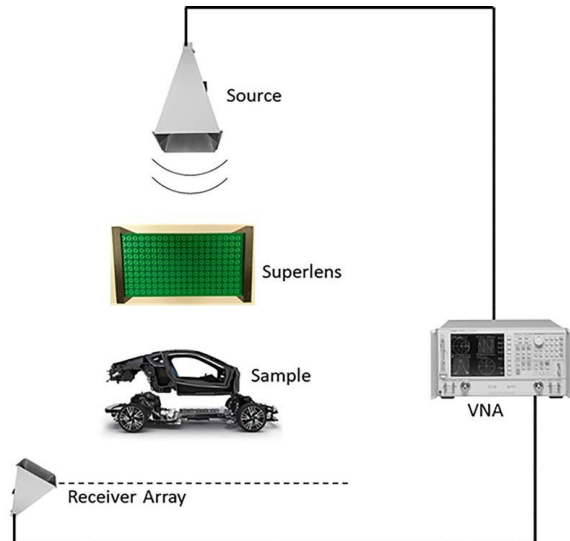


Fig. 2 Proposed microwave NDE imaging system using a metamaterial lens

conventional medium, Pendry demonstrated in Ref. [20] by using strictly causal calculations that these waves were amplified in metamaterials. This phenomenon of magnification of evanescent waves along with the perfect focusing nature of the superlens can be exploited for the detection of sub-wavelength defects. Figure 2 shows a schematic of the proposed NDE system with a metamaterial lens. Fields transmitted from the source are focused by the lens at the sample. The scattered fields from the defect will be stronger due to the focused fields and amplified evanescent waves in the presence of the lens. The scattered fields are captured by the receiver array through a vector network analyzer that will provide high-resolution information about the sample.

The negative refractive index of a metamaterial occurs due to the EM response of its periodic building blocks known as unit cells. The following section discusses the modeling of the unit cell of a metamaterial lens.

Theory and Unit Cell Design

Metamaterial Theory. An array of thin metallic wires with spacing in the order of millimeters behaves like an electric plasma in the GHz regime [21]. The variation of dielectric permittivity ϵ of an electric plasma as a function of frequency ω is given by

$$\epsilon(\omega) = 1 - \frac{\omega_p^2}{\omega(\omega + i\gamma)} \quad (3)$$

where ω_p is the plasma frequency and γ is the damping factor for dissipation. Equation (3) essentially indicates that $\epsilon(\omega)$ is negative

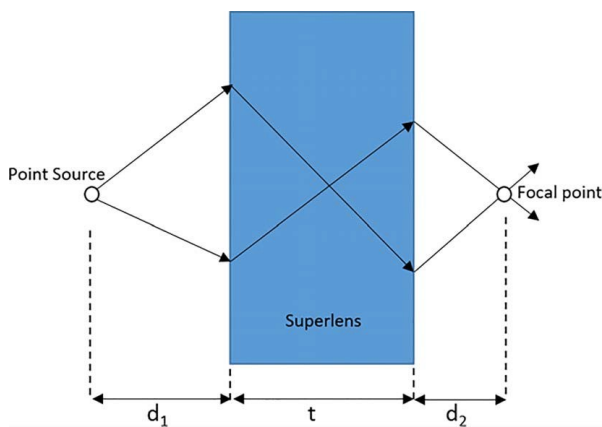


Fig. 1 Ray diagram of a superlens

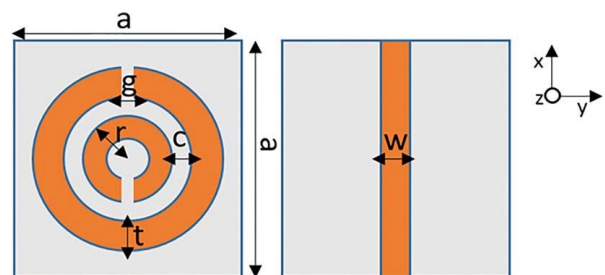


Fig. 3 Unit cell design

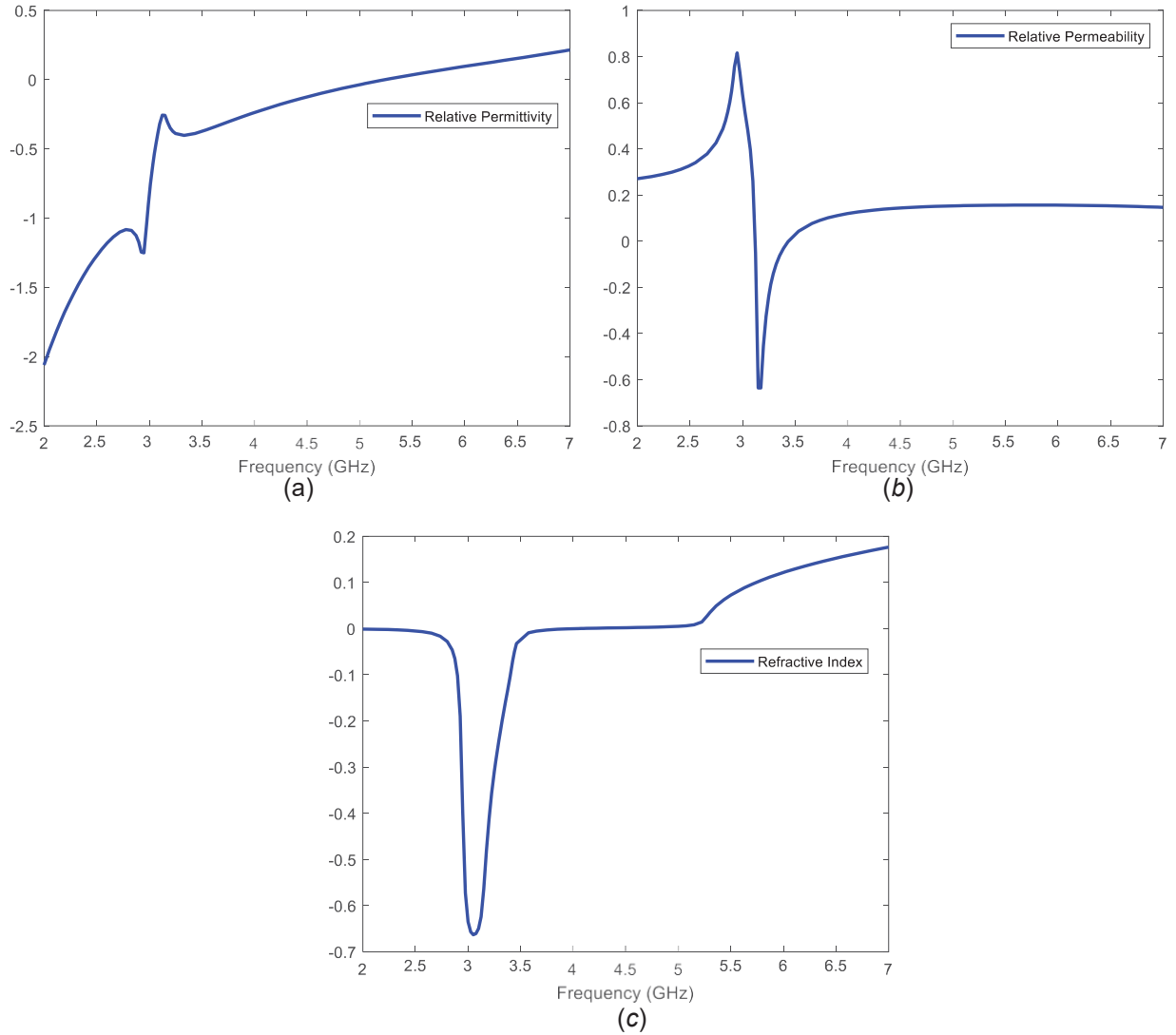


Fig. 4 Simulation results for electromagnetic parameters: (a) refractive index, (b) permittivity, and (c) permeability as a function of frequency

below plasma frequency. The array of wires behaves as a negative electric permittivity material at these frequencies.

In Ref. [22], it was proposed that an array of conducting loops or rings can mimic a magnetic plasma at microwave frequencies. The variation of magnetic permeability μ of a magnetic plasma as a function of frequency ω is given by

$$\mu(\omega) = 1 - \frac{F\omega^2}{\omega^2 - \omega_0^2 + i\gamma\omega} \quad (4)$$

where ω_0 is the resonant frequency and F is the fractional volume of the unit cell occupied by the loop. Equation 4 indicates that $\mu(\omega)$ is positive for frequencies up to the resonant frequency ω_0 and thereafter $\omega = \omega_0 / \sqrt{1 - F}$. The array of conducting rings behaves as a negative magnetic permeability material in this frequency region.

Unit Cell Design

Combining both the wire and ring structures in a periodic manner gives rise to materials having the unique property of simultaneously negative permittivity and permeability (double negative medium). The dimensions of the unit cell representing the metamaterial periodic array structure must be much smaller than the operating

wavelength to act as an effective medium. This is a required condition for the EM waves to physically interact with the lens as a homogenous medium with distinct macroscopic properties of effective permittivity and permeability. Figure 3 shows the unit cell design of the metamaterial lens comprising thin parallel wires and split ring resonators (SRRs). The unit cell is designed to operate around 3.5 GHz. The dimensions of the unit cells are as follows: $a = 9.3$ mm, $r = 2.5$ mm, $t = w = 0.9$ mm, and $g = c = 0.2$ mm.

Results and Discussion

Simulation Studies. Initial numerical studies using finite element EM solver ANSYS HFSS demonstrate the negative refractive index behavior of the lens. The electric field was polarized parallel to the wires (x -direction in Fig. 3) while the magnetic field was polarized normal to the surface of the unit cell (z -direction) and both are perpendicular to the direction of wave propagation (y -direction). Periodic boundary conditions were implemented to simulate an infinite array of SRRs and wires. The scattering parameters obtained from the full-wave simulations were used for the extraction of EM parameters, namely, permittivity, permeability, and refractive index of the metamaterial design [23]. The extracted

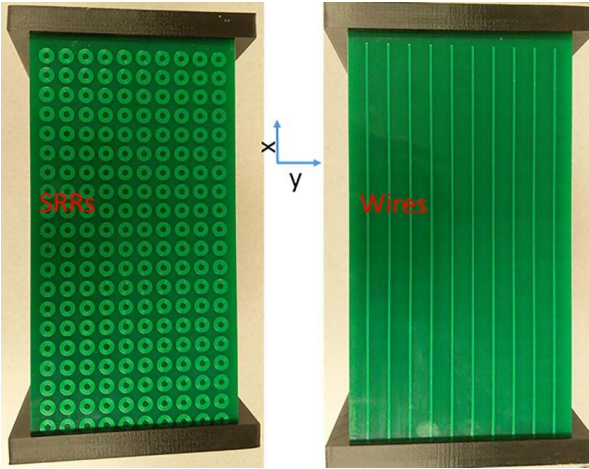


Fig. 5 Fabricated metamaterial lens

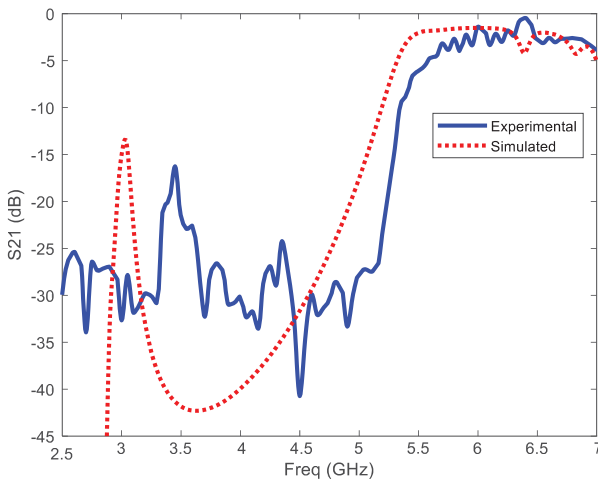


Fig. 6 Comparison of normalized transmission response of lens (experimental and simulated)

parameters are shown in Fig. 4. The permittivity and permeability curves have forms as depicted in Eqs. (3) and (4). The parameters are simultaneously negative around the resonant frequency of 3.5 GHz which makes the refractive index negative for the material in that regime (1). The lowest value of the refractive index (-0.66) occurs at 3.1 GHz.

Experiment. After simulation of the unit cell and extraction of its constitutive properties, the lens was fabricated for experimental validation. Figure 5 shows the fabricated lens. It has 20×10 unit cells in one layer (in the $x-y$ plane) and 30 such layers in the z -direction with a spacing of 6.5 mm.

Two wideband Vivaldi antennas (675 MHz to 12,000 MHz) were used as transmitter and receiver for obtaining the scattering parameters of the lens. Vivaldi antennas were chosen to ensure the correct field polarization that is required to achieve the negative properties as discussed in the ‘‘Simulation Studies’’ subsection. The normalized transmission characteristics obtained from vector network analyzer are plotted in Fig. 6. The experimental data closely follows the simulated curve. Waves inhibited in a negative μ and negative ϵ material are allowed to propagate in a double negative medium. The electric field, magnetic field, and direction of propagation of such waves form a left-handed triplet of vectors instead of the conventional right-handed one [24]. Such a left-handed passband is observed around 3.5 GHz. The passband

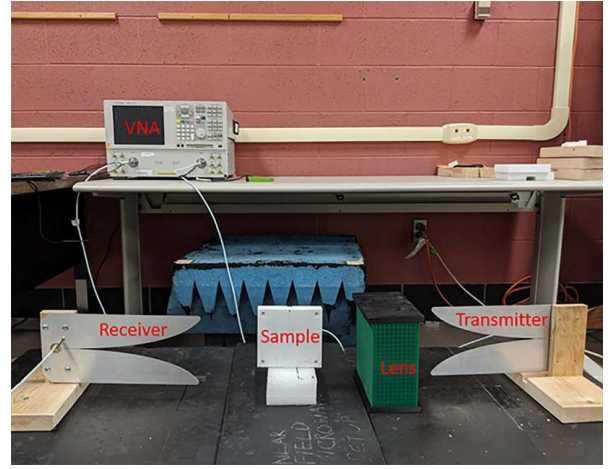


Fig. 7 Experimental setup of microwave NDE imaging system using a metamaterial lens

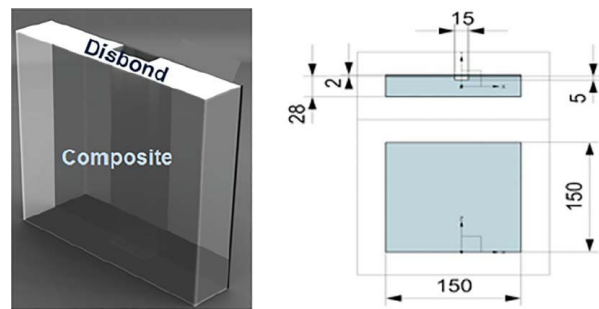


Fig. 8 Schematic diagram of sample geometry

Table 1 Samples under test

Sample	Dimensions ($x-y-z$)	Groove width and depth
Healthy	150 mm \times 150 mm \times 28 mm	NA
Large defect	150 mm \times 150 mm \times 28 mm	30 mm \times 10 mm
Small defect	150 mm \times 150 mm \times 28 mm	15 mm \times 5 mm

is due to the simultaneous stop bands caused by the negative μ and ϵ of the SRRs and wires media, respectively, at that frequency. At frequencies higher than 5.5 GHz, both the wires and SRRs allow normal transmission of EM waves.

Imaging results demonstrating the idea of sub-wavelength resolution with time-reversal processing using the superlens was presented in Ref. [18]. The concept was studied using EM finite difference time domain simulations considering a homogenized double negative layer as the metamaterial lens. The experimental study of enhancing microwave detection capability using the fabricated lens is presented in the following section.

Teflon samples with a machined groove along the length to mimic disbands in metal-composite joints were used as test samples. The experimental setup is shown in Fig. 7, and the schematic of the sample and defect dimensions are shown in Fig. 8. Three samples were tested with two sets of reading from each sample. The first set of readings was in free space without the lens while the second set of measurements was taken with the lens. The three samples under test are summarized in Table 1.

The transmission characteristics for the samples without and with the lens are shown in Figs. 9(a) and 9(b), respectively. The free space measurements show negligible differences between the

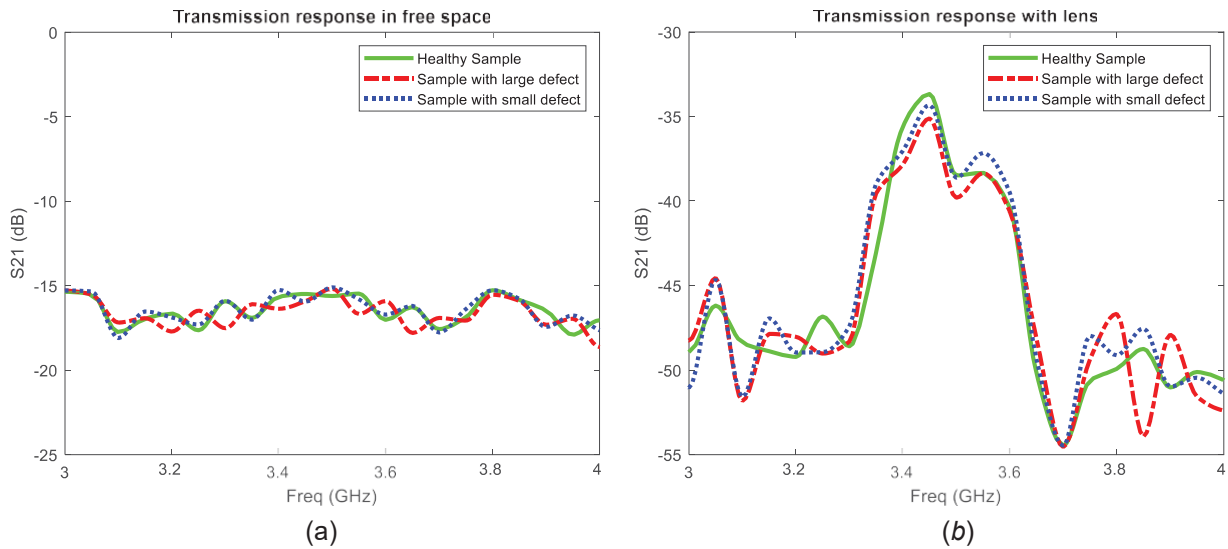


Fig. 9 Transmission response obtained using the experimental setup: (a) free space and (b) metamaterial lens

Table 2 Insertion loss with lens for different samples under test

Sample	S21 (dB)
Healthy	-33.67
Small defect	-34.32
Large defect	-35.12

three samples. The defect-free sample and the sample with smaller defect overlap for most of the frequency range. However, in the case of measurement with the lens, we observe a clear trend at the left-handed transmission peak at 3.44 GHz. The amplitude of the peak differs for the three samples. The values of the transmission peak are summarized in Table 2. The sample with a larger defect shows a greater change relative to the sample with a small defect. This is due to the fact that the scattering of waves from a larger defect would result in lower power received at the receiver. Such a trend is observed which shows the feasibility of enhancing far-field detection capability of a microwave system using a metamaterial lens.

Conclusion

This work discusses the physical design of a metamaterial lens for use in a microwave NDE setup. Modeling of the unit cell and extraction of its constitutive parameters has been presented. Simulation studies show the left-handed nature of the lens design, which is the basis of our proposed work. Prior research by the authors on numerical modeling of the NDE system comprising a source, receiver, and composite sample along with the lens, modeled as a homogeneous material, was done to determine its feasibility for sub-wavelength defect detection. This research focuses on the theoretical design of the discrete, periodic structures which describe the physical metamaterial lens. Fabrication of the lens, experimental validation of left-handed transmission, and feasibility of enhancing far-field microwave detection were presented. Future work involves further characterization of the fabricated lens. The prospects, as well as limitations of detecting sub-wavelength defects using the actual lens design, need to be studied extensively. Finally, work on the building of a microwave scanning system integrating the metamaterial lens is in progress to transcend the diffraction theory limits in conventional imaging systems.

Acknowledgment

This work was supported by the National Science Foundation through Manufacturing USA program with award number 1762331.

Nomenclature

n = refractive index
 μ = permeability
 ϵ = permittivity

References

- [1] Ku, H., Wang, H., Pattrachaiyakop, N., and Trada, M., 2011, "A Review on the Tensile Properties of Natural Fiber Reinforced Polymer Composites," *Composites, Part B*, 42(4), pp. 856–873.
- [2] Mohammed, L., Ansari, M. N. M., Pua, G., Jawaid, M., and Saiful Islam, M., 2015, "A Review on Natural Fiber Reinforced Polymer Composite and Its Applications," *Int. J. Polym. Sci.*, 2015, pp. 1–15.
- [3] Soutis, C., 2005, "Fibre Reinforced Composites in Aircraft Construction," *Prog. Aerosp. Sci.*, 41(2), pp. 143–151.
- [4] Senthil, K., Arockiarajan, A., Palaminathan, R., Santhosh, B., and Usha, K. M., 2013, "Defects in Composite Structures: Its Effects and Prediction Methods—a Comprehensive Review," *Compos. Struct.*, 106, pp. 139–149.
- [5] Bray, D. E., and Stanley, R. K., 1996, *Nondestructive Evaluation: a Tool in Design, Manufacturing and Service*, CRC Press, Boca Raton, FL.
- [6] Bahr, A. J., 1995, "Experimental Techniques in Microwave NDE," *Review of Progress in Quantitative Nondestructive Evaluation*, Vol. 14, D. O. Thompson, and D. E. Chimenti, eds., Springer, Boston, MA.
- [7] Kharkovsky, S., and Zoughi, R., 2007, "Microwave and Millimeter Wave Nondestructive Testing and Evaluation—Overview and Recent Advances," *IEEE Instru. Meas. Mag.*, 10(2), pp. 26–38.
- [8] Li, Z., Haigh, A., Soutis, C., and Gibson, A., 2018, "Principles and Applications of Microwave Testing for Woven and non-Woven Carbon Fibre-Reinforced Polymer Composites: a Topical Review," *Appl. Compos. Mater.*, 25(4), pp. 965–982.
- [9] Balanis, C. A., 2005, *Antenna Theory: Analysis and Design*, 3rd ed., Wiley, Hoboken, NJ, pp. 34.
- [10] Mukherjee, S., Tamburrino, A., Haq, M., Udupa, S., and Udupa, L., 2018, "Far Field Microwave NDE of Composite Structures Using Time Reversal Mirror," *NDT&E Int.*, 93, pp. 7–17.
- [11] Mukherjee, S., Shi, X., Udupa, L., Udupa, S., Deng, Y., and Chahal, P., 2018, "Design of a Split-Ring Resonator Sensor for Near-Field Microwave Imaging," *IEEE Sens. J.*, 18(17), pp. 7066–7076.
- [12] Grbic, A., and Eleftheriades, G. V., 2004, "Overcoming the Diffraction Limit with a Planar Left-Handed Transmission-Line Lens," *Phys. Rev. Lett.*, 92(11), p. 117403.
- [13] Aydin, K., Bulu, I., and Ozbay, E., 2007, "Subwavelength Resolution With a Negative-Index Metamaterial Superlens," *Appl. Phys. Lett.*, 90(25), p. 254102.
- [14] Ozbay, E., Li, Z., and Aydin, K., 2008, "Super-resolution Imaging by one-Dimensional, Microwave Left-Handed Metamaterials with an Effective Negative Index," *J. Phys.: Condens. Matter*, 20(30), pp. 304216.

[15] Savin, A., Bruma, A., Steigmann, R., Iftimie, N., and Faktorova, D., 2015, "Enhancement of Spatial Resolution Using a Metamaterial Sensor in Nondestructive Evaluation," *Appl. Sci.*, 5(4), pp. 1412–1430.

[16] Zhang, Y., Zhao, J., Cao, J., and Mao, B., 2018, "Microwave Metamaterial Absorber for non-Destructive Sensing Applications of Grain," *Sensors*, 18(6), p. 1912.

[17] Shreiber, D., Gupta, M., and Cravey, R., 2011, "Comparative Study of 1-D and 2-D Metamaterial Lens for Microwave Nondestructive Evaluation of Dielectric Materials," *Sens. Actuators, A*, 165(2), pp. 256–260.

[18] Mukherjee, S., Su, Z., Udpa, L., Udpa, S., and Tamburino, A., 2019, "Enhancement of Microwave Imaging Using a Metamaterial Lens," *IEEE Sens. J.*, 19(13), pp. 4962–4971.

[19] Veselago, V. G., 1968, "The Electrodynamics of Substances with Simultaneously Negative Values of and μ ," *Phys.-Usp.*, 10(4), pp. 509–514.

[20] Pendry, J. B., 2000, "Negative Refraction Makes a Perfect Lens," *Phys. Rev. Lett.*, 85(18), pp. 3966–3969.

[21] Pendry, J. B., Holden, A. J., Stewart, W. J., and Youngs, I., 1996, "Extremely low Frequency Plasmons in Metallic Mesostructures," *Phys. Rev. Lett.*, 76(25), pp. 4773–4776.

[22] Pendry, J. B., Holden, A. J., Robbins, D. J., and Stewart, W. J., 1999, "Magnetism From Conductors and Enhanced Nonlinear Phenomena," *IEEE Trans. Microwave Theory Tech.*, 47(11), p. 2075.

[23] Smith, D. R., Vier, D. C., Koschny, T., and Soukoulis, C. M., 2005, "Electromagnetic Parameter Retrieval From Inhomogeneous Metamaterials," *Phys. Rev. E*, 71(3), p. 036617.

[24] Smith, D. R., Padilla, W. J., Vier, D. C., Nemat-Nasser, S. C., and Schultz, S., 2000, "Composite Medium With Simultaneously Negative Permeability and Permittivity," *Phys. Rev. Lett.*, 84(18), pp. 4184–4187.